Catal Lett (2008) 126:353–360
DOI 10.1007/s10562-008-9630-2

Positive Effect of Water Vapor on CO Oxidation at Low Temperature over $Pd/CeO_2–TiO_2$ Catalyst

Feixue Liang · Huaqing Zhu · Zhangfeng Qin ·
Hui Wang · Guofu Wang · Jianguo Wang

Received: 8 July 2008 / Accepted: 27 August 2008 / Published online: 23 September 2008

Abstract CO oxidation at low temperature over $Pd/CeO_2–TiO_2$ catalyst was carried out in the feed containing different contents of water vapor (H_2O). A positive effect of H_2O was observed on the catalytic performance of $Pd/CeO_2–TiO_2$ in CO oxidation at low temperature. The extent of this effect depends on the content of H_2O in the feed; with a H_2O content being 2.5 vol%, the catalyst $Pd/CeO_2–TiO_2$ exhibits the highest stability (longest life time for CO oxidation at 80 °C). The results of in situ diffuse reflectance infrared Fourier transform spectroscopy (DRIFTS) and temperature-programmed reaction (TPReaction) reaction illustrated that H_2O in the feed supplies sufficient OH groups in the presence of O_2, which can react with adsorbed CO on Pd species to produce CO_2. Moreover, H_2O may also enhance the adsorption of CO and suppress the formation of some carbonate species.

Keywords Carbon monoxide oxidation · Low temperature · $Pd/CeO_2–TiO_2$ · Water vapor · DRIFTS · TPReaction

1 Introduction

The catalytic oxidation of CO at low temperature has attracted considerable attention because of its wide applications in the exhaust abatement for CO_2 lasers, trace CO removal in enclosed atmospheres, automotive emission control, and CO preferential oxidation (COPROX) for proton exchange membrane fuel cells (PEMFC) [1]. For a practical application of CO catalytic oxidation, the feedstock often contains inevitably certain amounts of water vapor (H_2O). Although many efforts have been made to investigate the effects of H_2O on CO oxidation, there are still a lot of controversies on clarifying the function of H_2O in CO oxidation. Positive effects of H_2O were ever claimed for Au/TiO_2 [2], Au/Fe_2O_3 [2–4], Au/CeO_2 [5], Au/Al_2O_3 [2, 6], $Pt/\gamma\text{-}Al_2O_3$ [3, 7], Pt/SnO_2 [8], $Pt–Mg/Al_2O_3$ [9], $Pt–Pd/CeO_2$ [10] and $Pd/CeO_2/ZrO_2$ [11] catalysts. On the other hand, however, negative effects of H_2O were reported for Au/TiO_2 [12], $Au/TiO_2–In_2O_3$ [12], Ru/C and Pt/C (porous carbonaceous material) [13], $Pd–Fe–O_x/NaZSM\text{-}5$ [14], CuO/CeO_2 [3, 15, 16] and CeO_2-promoted $Cu/\gamma\text{-}Al_2O_3$ catalysts [17].

For Au catalysts, both positive and negative effects of H_2O on CO oxidation or COPROX in H_2-rich stream were reported. Grunwaldt et al. [18] reported a reduced activity over Au/TiO_2 for low temperature CO oxidation when 0.1 vol% H_2O was presented in the reaction atmosphere, but this negative effect was easily reverted by simply switching to a dry mixture. Nevertheless, Daté and coworkers [19, 20] reported that the effect of H_2O on the catalytic performance of Au/TiO_2 in CO oxidation is strongly dependent on the moisture content in the feed; a low content of H_2O (0.1–200 ppm) was beneficial to CO oxidation, while higher H_2O content (ca. 6,000 ppm) brought on a decrease in the catalytic activity. In contrast, Schubert et al. [21] reported a positive effect of H_2O addition on the selective CO oxidation in H_2-rich gases over $Au/\alpha\text{–}Fe_2O_3$; H_2O may promote CO oxidation and suppress the competitive H_2 oxidation. Meanwhile, the deactivation was significantly diminished due to the

---

F. Liang · H. Zhu · Z. Qin · H. Wang · G. Wang · J. Wang (✉)
State Key Laboratory of Coal Conversion, Institute of Coal Chemistry, Chinese Academy of Sciences, P.O. Box 165,
Taiyuan, Shanxi 030001, China
e-mail: iccjgw@sxicc.ac.cn

F. Liang · H. Wang
Graduate University of the Chinese Academy of Sciences,
Beijing 100049, China

transformation of surface carbonates into thermally less stable bicarbonate species.

For Pt catalysts, the effect of H_2O on the CO oxidation or COPROX in H_2-rich gases was depended on the types of the supports. With metal oxides (Al_2O_3 [3, 7, 22], SnO_2 [8], etc.) as supports, the positive effect of H_2O on CO oxidation or COPROX in H_2-rich stream predominated in the known reports. The existence of H_2O dramatically enhanced CO conversion on Pt/γ-Al_2O_3 catalyst in the range of 110–190 °C, and reduced the activation energy for CO oxidation to about 37 kJ from 74 kJ in the absence of H_2O [22]. On the other hand, the negative effect of H_2O was observed on some porous materials [13] supported Pt catalysts. Snytnikov et al. [13] reported that the outlet CO concentration for CO selective oxidation over Ru/C and Pt/C catalysts increased with the addition of H_2O in the feed; this might be relevant to the blockage of catalyst active sites by H_2O adsorption as well as to the formation of CO–H_2O surface complexes that were less active than the adsorbed CO.

For non-noble metal catalysts, especially Cu–Ce based catalysts, only negative effect of H_2O on CO oxidation or COPROX in H_2-rich stream was found in the literatures [15–17], which was generally accused to the blocking of active sites on the catalyst by H_2O adsorption.

It is noteworthy that supported Pd catalyst also performs well in CO oxidation; however, few researches about the effects of H_2O in the feed (especially with different H_2O contents) on CO oxidation over Pd catalysts have been reported. In our previous work, Pd supported on the ceria–titania composite oxides (Pd/CeO_2–TiO_2) prepared by the method of sol–gel precipitation followed by supercritical fluid dry (SCFD) exhibited high activity for CO oxidation in a moisture-free atmosphere at low temperature [23]. Further works on the temperature-programmed reduction (TPR) using H_2 and CO as reducing agents suggested that the Pd–Ce interaction in Pd/CeO_2–TiO_2 favored the reduction of both PdO and CeO_2, which contributed to the high activity for CO oxidation at low temperature [24–26]. These works also suggested that the pretreatments of calcination and reduction might exhibit significant effects on the catalytic behavior of Pd/CeO_2–TiO_2 [27, 28]. To evaluate whether Pd/CeO_2–TiO_2 can still perform well in CO oxidation under the relatively actual conditions, it is essential to investigate the influence of H_2O on the CO oxidation behaviors.

In this work, an effort was made to investigate the effect of H_2O on the catalytic performance of Pd/CeO_2–TiO_2 in CO oxidation at low temperature. For this purpose, CO oxidation at low temperature over Pd/CeO_2–TiO_2 catalyst was carried out in the feed containing different contents of H_2O. In addition, in situ diffuse reflectance infrared Fourier transform spectroscopy (DRIFTS) and temperature-programmed reaction (TPReaction) were used to elucidate the role of H_2O in the process of CO oxidation.

2 Experimental

2.1 Catalyst Preparation

The catalyst Pd/CeO_2–TiO_2 was prepared in the similar procedures as described previously [24, 27, 28]. Briefly, CeO_2–TiO_2 support was prepared through sol–gel precipitation with $TiCl_4$ and $Ce(NO_3)_3 \cdot 6H_2O$ as precursors. After aging, washing and exchanging water with pure ethanol, the precipitate was dried at 120 °C for 24 h and calcined at 500 °C in air for 3 h. Pd supported catalyst was prepared by incipient wetness impregnation of CeO_2–TiO_2 with aqueous $PdCl_2$ solution. In this work, Ti/Ce atomic ratio is 5.0 for the CeO_2–TiO_2 support and Pd loading is 1.0 wt% for the Pd/CeO_2–TiO_2 catalyst.

2.2 Catalytic Tests and Analytic Procedures

The catalytic tests for CO oxidation over Pd/CeO_2–TiO_2 catalyst were carried out in a quartz tubular flow micro reactor with an internal diameter of 6.0 mm at atmospheric pressure, with the similar procedures described previously [27, 28]. Briefly, about 200 mg of catalyst sample (40–60 mesh) was used per run; the catalyst bed was about 1.0 cm in height and placed in the constant temperature zone (3–4 cm high) of the micro reactor and embedded between glass wool plugs. Prior to the measurement, the catalysts underwent an on-line pre-reduction in hydrogen (50 ml/min) at 150 °C, namely, low temperature reduction (LTR) pretreatment.

Light-off test of CO oxidation was conducted from room temperature (RT) at a heating rate of 1.0 °C min^{-1}; long-term stability of Pd/CeO_2–TiO_2 was examined at 80 °C. The reaction stream consisted of 1.0 vol% CO and 5.0 vol% O_2 balanced with argon; GHSV was 45,000 ml g^{-1} h^{-1} ($W/F = 0.080$ g s cm^{-3}). A bubbler saturator was used to introduce H_2O into the feed and the content of H_2O in the feed was controlled by the evaporating temperature. The gas line leading to the reactor was heated and kept at 120 °C to avoid any H_2O condensation.

The effluent gas from the reactor was periodically analyzed online with a gas chromatograph (SHIMADZU GC-8A) equipped with a 3 mm × 2 m stainless-steel column packed with carbon molecular sieve, a post-column methanator that converted CO and CO_2 into CH_4, and a flame ionization detector (FID).

2.3 Catalyst Characterization

In situ DRIFTS of CO adsorption and oxidation were carried out on a Nicolet 380 FT-IR spectrometer equipped with a MCT/A detector at a spectral resolution of 4 cm^{-1} (accumulating 32 scans). About 40 mg of the powder catalyst was placed in the diffuse reflectance cell and underwent an on-line LTR pretreatment. The background spectra were recorded in a flow of pure argon just prior to the measurement. The spectra were collected at 80 °C after the catalyst sample was exposed to the corresponding reactive stream (30 ml min^{-1}, $W/F = 0.080$ g s cm^{-3}) for about 20 min. For CO adsorption, the stream was 5.0 vol% CO and 2.6 vol% H_2O (when used) with balanced argon; for CO oxidation, it contained 1.0 vol% CO, 5.0 vol% O_2 and 2.8 vol% H_2O (when used) with balanced argon.

TPReaction between CO and H_2O over Pd/CeO_2–TiO_2 was performed in the same quartz micro reactor as used in the catalytic tests. Here, about 100 mg of catalyst sample was used in each run; CO, H_2O, CO_2 and H_2 in the outlet gas were measured on-line by a quadrupole mass spectrometer (QMS, OmniStar^{TM}) instead. The catalyst sample was first pretreated following the aforementioned LTR procedure. After that, the catalyst sample was cooled down to RT under an argon flow (50 ml min^{-1}), and then the argon stream was shifted to a reacting stream of 5.0 vol% CO and 2.6 vol% H_2O in argon at a GHSV of 30,000 ml g^{-1} h^{-1} ($W/F =$ 0.12 g s cm^{-3}). After a stable composition in the outlet gas was attained, the TPReaction profiles of each component were recorded from RT to 500 °C with a heating rate of 10 °C/min.

3 Results and Discussion

3.1 Catalyst Textural Properties

As reported previously [29], BET surface area of the composite CeO_2–TiO_2 as prepared is 207.9 m^2 g^{-1}. By comparison, the surface areas of single TiO_2 and CeO_2 prepared using the same procedure are only 62.9 and 108.6 m^2 g^{-1}, respectively. TEM images of CeO_2, TiO_2 and CeO_2–TiO_2 suggested that CeO_2–TiO_2 has lost the appearance of both CeO_2 and TiO_2. The powder XRD patterns showed that CeO_2–TiO_2 composite oxide is in an amorphous structure; a solid solution of CeO_2–TiO_2 may be formed with Ti^{4+} replacing Ce^{4+} into the CeO_2 lattice or its precursor [24].

The XRD pattern of Pd/CeO_2–TiO_2 is almost the same as that of CeO_2–TiO_2, which proves that the preparation of Pd/CeO_2–TiO_2 through impregnation and calcination does not cause any recrystallization of CeO_2–TiO_2 support. PdO phase is not observed in the XRD patterns of the Pd supported catalyst, indicating that either PdO is present as a non-crystalline phase or finely dispersed on the supports with the particle size being smaller than 3 nm [24, 29].

3.2 Effect of H_2O on the Performance of Pd/CeO_2–TiO_2 for CO Oxidation

To examine the effect of moisture on the CO oxidation over Pd/CeO_2–TiO_2, the light-off profiles of CO oxidation on the Pd/CeO_2–TiO_2 catalyst under dry and wet conditions are compared in Fig. 1. A positive effect of H_2O on the catalytic activity of Pd/CeO_2–TiO_2 in CO oxidation at low temperature is observed; to achieve a complete CO conversion, the catalyst needs much lower temperature in the presence of H_2O than in the absence of H_2O.

Long-term stability tests were carried out at 80 °C in the reaction stream (1.0 vol% CO + 5.0 vol% O_2 + balanced argon) containing different contents of H_2O. As shown in Fig. 2, the presence of 1.1–10.2 vol% H_2O in the reaction stream prolongs the life of Pd/CeO_2–TiO_2 catalyst in CO oxidation, especially with a H_2O content of 2.5 vol%. The prolongation of catalyst life time by H_2O is dependent on the H_2O content in the feed (in the order of $2.5 > 1.1 > 5.1 > 10.2$ vol%). By introducing 2.5 vol% H_2O into the feed, the catalytic stability is enhanced most significantly; the duration for CO conversion decreasing from 100.0 to 95.1% extends from only 0.43 h in the absence of H_2O to about 49.50 h.

Current results then strongly suggest that the presence of H_2O in the feed has a positive effect on the catalytic performance of Pd/CeO_2–TiO_2 in CO oxidation at low temperature. With a H_2O content being 2.5 vol% in the feed at the established conditions, this effect is most significant; the catalyst Pd/CeO_2–TiO_2 exhibits much higher stability (longer life time for CO oxidation at 80 °C) than that in the absence of H_2O.

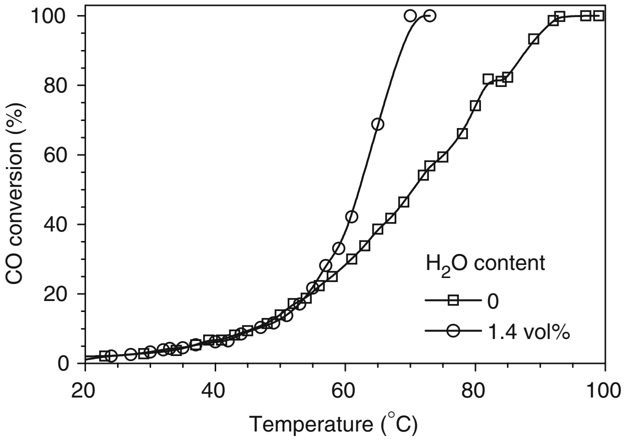

Fig. 1 Light-off profiles of Pd/CeO_2–TiO_2 in CO oxidation under dry and wet conditions in the reaction stream of CO 1.0, 5.0 vol% O_2 and balanced argon, GHSV = 45,000 h^{-1}

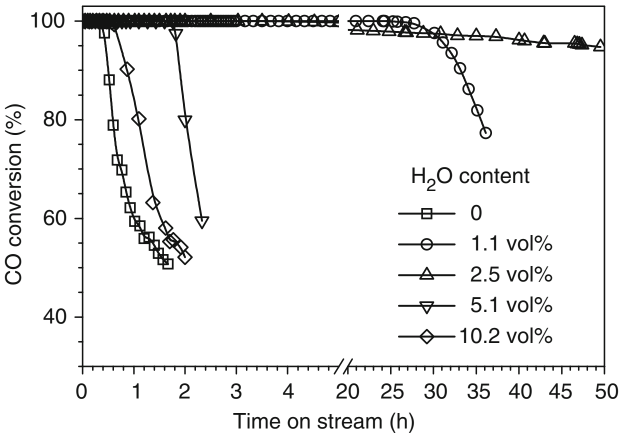

Fig. 2 Catalytic stability of Pd/CeO_2–TiO_2 in CO oxidation at 80 °C with different H_2O contents in the reaction stream of 1.0 vol% CO, 5.0 vol% O_2 and balanced argon, GHSV = 45,000 h^{-1}

3.3 In situ DRIFTS of CO Adsorption and Oxidation on Pd/CeO_2–TiO_2

To estimate the influence of H_2O on CO adsorption and oxidation on the LTR-pretreated Pd/CeO_2–TiO_2 catalyst, the DRIFTS spectra of CO adsorption in a 5.0 vol% CO/Ar flow both in the absence and presence of 2.6 vol% H_2O as well as CO oxidation in a 1.0 vol% CO + 5.0 vol% O_2 flow (balanced with Ar) both in the absence and in the presence of 2.8 vol% H_2O are obtained at 80 °C, as shown in Fig. 3.

The O–H stretching vibration of H_2O and OH groups is located between 3,800 and 3,000 cm^{-1} (Fig. 3(1)). The ascriptions of the bands appeared in this region can be summarized as follows: (1) the band at 3,743 cm^{-1} is ascribed to free H_2O [30]; (2) the bands in 3,710–3,500 cm^{-1} region are related to the stretching vibration of ceria hydroxyl groups [31–34]; (3) the broad band at ca. 3,400 cm^{-1} is due to the physisorbed H_2O molecules bound by weak hydrogen bonds with each other and with OH groups on CeO_2 and TiO_2 surface [35]. It is noticed that certain physisorbed H_2O is formed during the LTR pretreatment even if no additional H_2O is introduced into the feed (Fig. 3(1a)). A negative band at ca. 3,400 cm^{-1} is accidentally detected for CO oxidation in the absence of H_2O (Fig. 3(1c)), but not observable in the process of CO adsorption in the absence/presence of H_2O (Fig. 3(1a, b)). These may suggest that the physisorbed H_2O on the support is consumed in the process of CO oxidation.

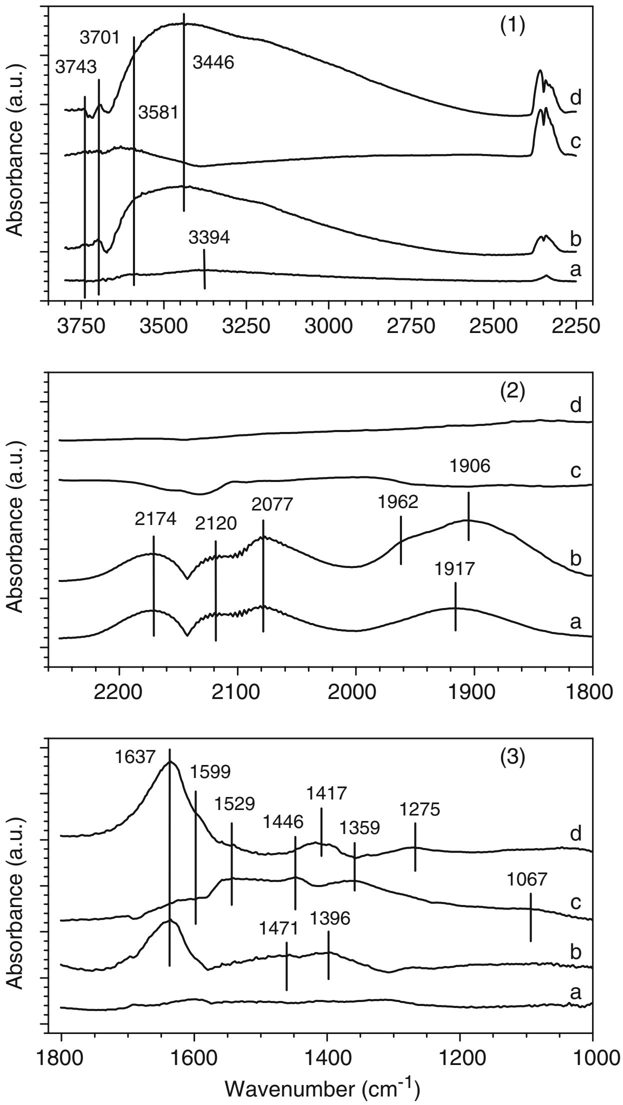

Fig. 3 DRIFTS spectra of CO adsorption and oxidation on Pd/CeO_2–TiO_2 at 80 °C in the atmospheres (balanced with argon) of (a) 5.0 vol% CO, (b) 5.0 vol% CO + 2.6 vol% H_2O, (c) 1.0 vol% CO + 5.0 vol% O_2, and (d) 1.0 vol% CO + 5.0 vol% O_2 + 2.8 vol% H_2O in the different regions: (1) H_2O and OH; (2) CO; and (3) carbonates

The absorption bands of gaseous CO_2 at 2,400–2,300 cm^{-1} are all detectable for CO adsorption and oxidation both in the absence and in the presence of H_2O (Fig. 3(1)). Because no gaseous CO_2 is introduced into the stream for DRIFTS measurements (gaseous CO_2 is not detected in the DRIFTS of H_2O adsorption alone), CO_2 detected for CO adsorption (Fig. 3(1a, b)) may be produced through two routes: (1) the reaction between CO and active oxygen provided by the support; (2) the reaction between CO and residual H_2O/OH groups on the support surface. The first route is supported by the fact that CeO_2 usually acts as an oxygen buffer by releasing-uptaking oxygen through redox processes involving the Ce^{4+}/Ce^{3+} couple in the catalyst [36]. However, H_2-TPR results reveal that only metallic Pd^0 and Ce^{3+} are present in the Pd/CeO_2–TiO_2 catalyst after LTR pretreatment [24, 26], indicating that the reaction between CO and oxygen species in CeO_2 on the support is negligible here for the formation of CO_2. Therefore, the gaseous CO_2 detected in the course of CO adsorption in the absence/presence of H_2O should be produced via the reaction between CO and H_2O/OH groups on the catalyst surface. Furthermore, because CO_2 is not formed from CO adsorption on $CeO_2–TiO_2$ support alone (not shown), the buildup of CO_2 here may originate from the CO adsorbed on Pd^0 and the reaction between CO and H_2O/OH then takes place on the interface of metal and support. The presence of H_2O in the feed supplies abundant H_2O/OH groups which react ulteriorly with CO on the surface of $Pd/CeO_2–TiO_2$ catalyst; this then leads to a significant increase of the CO_2 absorbance intensity in the DRIFTS spectra (Fig. 3(1a, b)). When introducing O_2 into the feed together with CO (either in the absence or in the presence of H_2O), CO_2 can then be produced through the aforementioned two routes (Fig. 3(1c, d)).

In the carbonyl region (2,250–1,800 cm^{-1}), as shown in Fig. 3(2), four bands are detected for DRIFTS of CO adsorption in the absence of H_2O; the bands at 2,174 and 2,120 cm^{-1} are related to gaseous CO [24], and the bands at 2,077 and 1,917 cm^{-1} should be ascribed to the linear and bridged CO adsorption on Pd^0, respectively (Fig. 3(2a)). With the presence of H_2O in the stream, both the linear and the bridged adsorption bands of CO on Pd^0 become more intense (Fig. 3(2b)). The band for CO bridged species at 1,917 cm^{-1} splits into two overlapped bands located at 1,906 and 1,962 cm^{-1}, which are together ascribed to the special CO bridged adsorbed structure [37]; they should be related to the active species for CO oxidation over $Pd/CeO_2–TiO_2$ in the presence of H_2O. These then support that the presence of H_2O improves the adsorption of CO on $Pd/CeO_2–TiO_2$ catalyst. An enhanced CO adsorption on the surface of gold particles in the presence of water was previously pointed out by Boccuzzi et al. [38], but little was known about how it occurred. When introducing O_2 into the stream both in the absence and in the presence of H_2O (Fig. 3(2c, d)), no carbonyl band is observable; this is in agreement with the high CO oxidation rate as shown in Fig. 2 that CO can be converted completely to CO_2 in the established conditions.

In the region of carbonate-like species (1,800–1,000 cm^{-1}), as shown in Fig. 3(3), the main ascriptions for the DRIFTS spectra are: (1) the band at 1,599 cm^{-1} is due to hydrogen carbonate species [32, 39]; (2) the band at 1,529 cm^{-1} is related to carboxylate species [40]; (3) the bands at 1,471, 1,446, 1,417, 1,396 and 1,359 cm^{-1} are related to unidentate carbonate species [41, 42]; (4) the band at 1,275 cm^{-1} corresponds to a kind of bidentate carbonate species [43]; (5) a broad band at 1,067 cm^{-1} is ascribed to internal polydentate carbonate [31, 43]. Moreover, after introducing H_2O into the stream (Fig. 3(3b, d)), an intense band appears at ca. 1,637 cm^{-1}, which should be attributed to the scissor-bending of free H_2O.

For CO adsorption in the absence of H_2O (Fig. 3(3a)), few carbonate species are formed on the surface of $Pd/CeO_2–TiO_2$ catalyst. When introducing H_2O into the feed together with CO, two bands at 1,471 and 1,396 cm^{-1} ascribed to the unidentate carbonate species are detected (Fig. 3(3b)).

For CO oxidation in the absence of H_2O, some intense bands for carbonate species are formed in this region. Besides two bands corresponding to the unidentate carbonate species at 1,446 and 1,359 cm^{-1}, hydrogen carbonate (e.g., 1,599 cm^{-1}), carboxylate species (e.g., 1,529 cm^{-1}) and polydentate carbonate species (e.g., 1,067 cm^{-1}) are also detected (Fig. 3(3c)). For CO oxidation in the presence of H_2O, however, the intensity of the bands in the carbonate region is prominently weakened by introducing H_2O (Fig. 3(3d)). The band at 1,599 cm^{-1} is overlapped by the band at 1,637 cm^{-1}. Two weak bands appear at 1,417 and 1,275 cm^{-1}; the former band should be ascribed to the unidentate carbonate species, while the latter one is corresponding to a kind of bidentate carbonate species. In comparison, some kinds of carbonate species are not detected in the presence of H_2O, which is in agreement with the results for Pd/CeO_2 reported by Hilaire et al. [39]. The presence of H_2O may suppress the accumulation of some kinds of carbonate species, which is favorable for CO oxidation; this may act as another crucial factor for the positive effect of H_2O on CO oxidation over $Pd/CeO_2–TiO_2$ catalyst.

3.4 TPReaction of CO and H_2O

To confirm the interaction between CO and H_2O on the catalyst surface at low temperature, TPReaction of CO and H_2O over LTR-pretreated $Pd/CeO_2–TiO_2$ catalyst is performed; the QMS signals of CO, H_2O, CO_2 and H_2 in the reactor outlet along with the temperature are shown in Fig. 4.

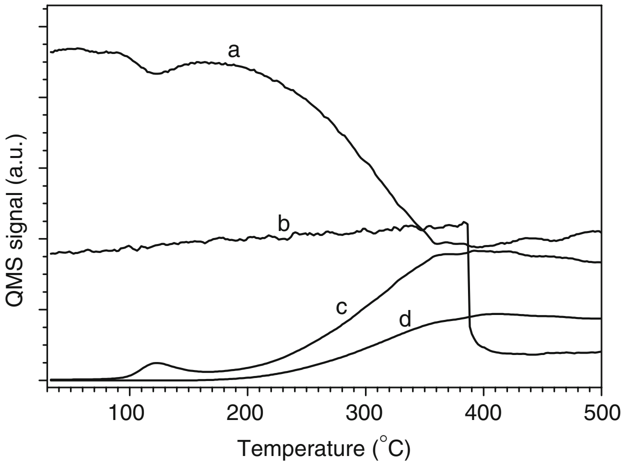

Fig. 4 TPReaction profiles of CO and H_2O over LTR-pretreated $Pd/CeO_2–TiO_2$ catalyst in a stream of 5.0 vol% CO + 2.6 vol% H_2O (balanced with argon) at a temperature from RT to 500 °C with a heating rate of 10 °C/min: (a) CO; (b) H_2O; (c) CO_2; and (d) H_2

CO consumption begins at about 75 °C, comes to a peak at 124 °C, speeds up from 161 °C, and then reaches a steady value at about 360 °C. The process of CO_2 production matches exactly that of CO consumption. However, H_2 production starts at a temperature higher than 170 °C and reaches a steady value at 360 °C. The first peak of CO consumption or CO_2 production at 124 °C corresponds to neither the formation of H_2 nor the consumption of H_2O. These can exclude the gaseous reaction between CO and H_2O at low temperature (<170 °C) and suggest that CO_2 is produced from the reaction of CO and OH group on the surface of $Pd/CeO_2–TiO_2$ catalyst:

$$\mathrm{CO + OH_s \rightarrow CO_2 + H_s} \tag{1}$$

where OH_s corresponds to the OH group originated from the support and H_s to hydrogen atom adsorbed on the support. On the other side, the water–gas shift between CO and H_2O only turns to be significant at a higher temperature (>200 °C).

3.5 Role of H_2O in Low Temperature CO Oxidation over LTR-pretreated $Pd/CeO_2–TiO_2$

For CO oxidation at low temperature over noble metal supported catalyst, it is generally accepted that noble metal is covered by CO, while O_2 is activated on the sites in the reducible supports or on the partially oxidized patches of reducible additives, such as Ce(ox) [44, 45], Sn(ox) [46] and Fe(ox) [47]. CO oxidation may follow a so-called bifunctional reaction pathway [48] at the noble metal/oxide interface; O_2 diffuses to the interface sites and reacts with CO adsorbed on the noble metal at its perimeter. The bi-functional path is also supported by the results of CO oxidation in the absence of H_2O over the reduced $Pd/CeO_2–TiO_2$ catalyst in our previous work [27], which involves the reaction between CO adsorbed on the noble metal and oxygen from ceria at the metal–ceria interface.

The catalytic tests in this work reveal a positive effect of H_2O on the catalytic performance of $Pd/CeO_2–TiO_2$ in CO oxidation at low temperature. The DRIFTS of CO adsorption in the presence of H_2O and TPReaction between CO and H_2O illustrate that H_2O may participate in the CO oxidation via the reaction between CO and OH groups whose formation is promoted by H_2O. On the basis of these observations, the following reaction pathways are then proposed to explain the role of H_2O in the CO oxidation over the LTR-pretreated $Pd/CeO_2–TiO_2$:

$$\mathrm{CO + Pd \leftrightarrow Pd - CO} \tag{2}$$

$$\frac{1}{2}\mathrm{O_2 + (OCeO[\ ]CeO)_s \leftrightarrow (OCeO[O]CeO)_s} \tag{3}$$

$$\mathrm{Pd - CO + (OCeO[O]CeO)_s \rightarrow Pd + CO_2 + (OCeO[\ ]CeO)_s} \tag{4}$$

$$\mathrm{H_2O_s + (OCeO[O]CeO)_s \leftrightarrow (OCeO[\ ]CeO)_s + 2OH_s} \tag{5}$$

$$\mathrm{Pd - CO} + OH_\mathrm{s} \rightarrow \mathrm{Pd + CO_2 + H_s} \tag{6}$$

$$\mathrm{H_s + (OCeO[O]CeO)}_s \rightarrow \mathrm{(OCeO[\ ]CeO)_s + H_2O} \tag{7}$$

where the symbol [ ] indicates the oxygen vacancy in Ce_2O_3, [O] denotes the oxygen captured and activated by the vacancy, and the suffix 's' means the support surface.

Reactions (2)–(4) represent the reaction pathway in the absence of H_2O as discussed in the reference [27], namely, the aforementioned bi-functional reaction pathway. Briefly, CO is adsorbed and activated on Pd^0 at the beginning (reaction (2)), while O_2 is captured and activated by the oxygen vacancy in the reduced ceria (reaction (3)). Then CO_2 is formed from the reaction between the adsorbed CO on Pd^0 and the captured oxygen by ceria at the metal–ceria interface (reaction (4)).

When H_2O is present in the feedstock, H_2O may take part in CO oxidation through the reactions (5)–(7). H_2O is generally adsorbed on the metal oxide support rather than on the precious metal [11]. The negative band at ca. 3,400 cm^{-1} for CO and O_2 coadsorption in Fig. 3(1c) suggests that CO oxidation consumes certain H_2O physisorbed on the supports. Besides, as the TPReaction tests confirmed (Fig. 4), the reaction temperature (80 °C) is so low that the water–gas shift reaction between CO and H_2O is negligible. It is then reasonable to presume that H_2O adsorbed on the support reacts with the captured oxygen in $(OCeO[O]CeO)_s$ to give OH groups (reaction (5)). After that, CO adsorbed on Pd species reacts with OH groups formed on the support to produce CO_2 through the reaction (6). Simultaneously, Hs is formed, which cannot combine together to release H_2 at current conditions due to the large amounts of O_2 in the stream. Instead of that, Hs may react with $(OCeO[O]CeO)_s$ to liberate H_2O and oxygen vacancy in Ce_2O_3 (reaction (7)).

As a whole, the presence of H_2O can supply abundant OH groups in the presence of O_2, and then OH groups react with the adsorbed CO on Pd species to produce CO_2. In this way, H_2O is thus helpful for O_2 activation; it also provides another route for CO oxidation (the reaction between CO and the H_2O/OH groups formed on the support surface) besides the route between CO and active oxygen in the absence of H_2O. These then bring on the positive effect on the catalytic performance of $Pd/CeO_2–TiO_2$ in CO oxidation at low temperature.

Meanwhile, H_2O may also promote the building of CO_2 as well as the leaving of CO_2 from the catalyst surface through reaction (6), which can suppress the accumulation of some kinds of carbonate species. The DRIFTS results prove that Pd/CeO_2–TiO_2 catalyst accumulates less carbonates for CO oxidation in the presence of H_2O than in the absence of H_2O (Fig. 3(3)). This will alleviate the catalyst deactivation due to the carbonate accumulation and prolong the catalyst life time, which acts as another crucial factor for the positive effect of H_2O on CO oxidation over Pd/CeO_2–TiO_2 catalyst.

On the other side, the blockage of active sites by H_2O adsorption on the catalyst can not be excluded when large amounts of H_2O are introduced in the feed. By taking account of both the negative side (blockage of active sites by H_2O adsorption) and the positive side (participation of H_2O in the CO oxidation and alleviation of the carbonate accumulation), the extent of H_2O positive effect on the performance of Pd/CeO_2–TiO_2 catalyst for CO oxidation then depends strongly on the H_2O content in the feed.

4 Conclusions

A positive effect of H_2O on the catalytic performance of Pd/CeO_2–TiO_2 in CO oxidation at low temperature is observed. The extent of this effect depends on the content of H_2O in the feed; with a H_2O content being 2.5 vol%, the catalyst Pd/CeO_2–TiO_2 exhibits the highest stability.

The DRIFTS of CO adsorption and oxidation in the absence/presence of H_2O and TPReaction between CO and H_2O suggest that H_2O participates in CO oxidation at low temperature indirectly by supplying abundant OH groups in the presence of O_2; OH groups then react with the adsorbed CO on Pd species to produce CO_2. In this way, H_2O may promote O_2 activation and then brings on the positive effect on low temperature CO oxidation over Pd/CeO_2–TiO_2.

Moreover, H_2O can enhance CO adsorption (both linear and bridged) and suppress the accumulation of certain carbonates, which may also contribute to the positive effect of H_2O on the catalytic performance of Pd/CeO_2–TiO_2 in CO oxidation at low temperature.

Acknowledgments The authors are grateful for the financial support of the State Key Fundamental Research Project (2007CB216401) and the Natural Science Foundation of China (20773155) and Shanxi Province (2007011037).

References

1. Yuan Y, Kozlova AP, Asakura K, Wan H, Tsai K, Iwasawa Y (1997) J Catal 170:191
2. Park ED, Lee JS (1999) J Catal 186:1
3. Avgouropoulos G, Ioannides T, Papadopoulou Ch, Batista J, Hocevar S, Matralis HK (2002) Catal Today 75:157
4. Neri G, Bonavita A, Rizzo G, Galvagno S, Donato N, Caputi LS (2004) Sens Actuat B 101:90
5. Romero-Sarria F, Penkova A, Martinez TLM, Centeno MA, Hadjiivanov K, Odriozola JA (2008) Appl Catal B doi:10.1016/j.apcatb.2008.03.010
6. Costello CK, Kung MC, Oh H-S, Wang Y, Kung HH (2002) Appl Catal A 232:159
7. Son IH, Lane AM, Johnson DT (2003) J Power Sources 124:415
8. Schryer DR, Upchurch BT, Van Norman JD, Brown KG, Schryer J (1990) J Catal 122:193
9. Cho SH, Park JS, Choi SH, Lee SK, Kim SH (2005) Catal Lett 103:257
10. Parinyaswan A, Pongstabodee S, Luengnaruemitchai A (2006) Int J Hydro Energy 31:1942
11. Rajasree R, Hoebink JHBJ, Schouten JC (2004) J Catal 223:36
12. Debeila MA, Wells RPK, Anderson JA (2006) J Catal 239:162
13. Snytnikov P, Sobyanin VA, Belyaev VD, Tsyrulnikov PG, Shitova NB, Shlyapin DA (2003) Appl Catal A 239:149
14. Bi Y, Chen L, Lu G (2007) J Mol Catal A 266:173
15. Avgouropoulos G, Ioannides T (2003) Appl Catal A 244:155
16. Avgouropoulos G, Ioannides T, Matralis H (2005) Appl Catal B 56:87
17. Shiau C-Y, Ma MW, Chuang CS (2006) Appl Catal A 301:89
18. Grunwaldt JD, Kiener C, Wögerbauer C, Baiker A (1999) J Catal 181:223
19. Dáte M, Haruta M (2001) J Catal 201:221
20. Dáte M, Ichihashi Y, Yamashita T, Chiorino A, Boccuzzi F, Haruta M (2002) Catal Today 72:89
21. Schubert MM, Venugopal A, Kahlich MJ, Plzak V, Behm RJ (2004) J Catal 222:32
22. Manasilp A, Gulari E (2002) Appl Catal B 37:17
23. Dong G, Wang J, Gao Y, Chen S (1999) Catal Lett 58:37
24. Zhu H, Qin Z, Shan W, Shen W, Wang J (2004) J Catal 225:267
25. Zhu H, Qin Z, Wang J (2005) Chin J Catal 26:377
26. Zhu H, Qin Z, Wang J (2004) J Fuel Chem Technol 32:729
27. Zhu H, Qin Z, Shan W, Shen W, Wang J (2005) J Catal 233:41
28. Zhu H, Qin Z, Shan W, Shen W, Wang J (2007) Catal Today 126:382
29. Liang F, Zhu H, Qin Z, Wang H, Wang G, Wang J (2008) Chin J Catal 29:264
30. Jacobs G, Williams L, Graham U, Sparks D, Davis BH (2003) J Phys Chem B 107:10398
31. Holmgren A, Andersson B, Duprez D (1999) Appl Catal B 22:215
32. Binet C, Daturi M, Lavalley JC (1999) Catal Today 50:207
33. Meunier FC, Tibiletti D, Goguet A, Reid D, Burch R (2005) Appl Catal A 289:104
34. Wang JA, Dominguez JM, Montoya A, Castillo S, Navarrete J, Moran-Pineda M, Reyes-Gasga J, Bokhimi X (2002) Chem Mater 14:4676
35. Bezrodna T, Puchkovska G, Shymanovska V, Baran J, Ratajczak H (2004) J Mol Struct 700:175
36. Trovarelli A (1996) Catal Rev Sci Eng 38:439
37. Choi KI, Vannice MA (1991) J Catal 127:465
38. Boccuzzi F, Chiorino A, Tsubota S, Haruta M (1995) Sens Actuat B 25:540
39. Hilaire S, Wang X, Luo T, Gorte RJ, Wagner J (2001) Appl Catal A 215:271
40. Bozon-Verduraz F, Bensalem A (1994) J Chem Soc Faraday Trans 90:653
41. Shido T, Iwasawa Y (1993) J Catal 141:71
42. Shido T, Asakura K, Iwasawa Y (1990) J Catal 122:55
43. Pozdnyakova O, Teschner D, Wootsch A, Kröhnert J, Steinhauer B, Sauer H, Toth L, Jentoft FC, Knop-Gericke A, Paál Z, Schlögl R (2006) J Catal 237:17
44. Wootsch A, Descorme C, Duprez D (2004) J Catal 225:259

45. Özkara S, Aksoylu AE (2003) Appl Catal A 251:75
46. Schubert MM, Kahlich MJ, Feldmeyer G, Hüttner M, Hackenberg S, Gasteiger HA, Behm RJ (2001) Phys Chem Chem Phys 3:1123
47. Liu X, Korotkikh O, Farrauto R (2002) Appl Catal A 226:293
48. Nibbelke RH, Nievergeld AJL, Hoebink JHBJ, Marin GB (1998) Appl Catal B 19:245